FORCE SPECTROSCOPY

Molecular force spectroscopy with a DNA origami–based nanoscopic force clamp

Philipp C. Nickels,[1] Bettina Wünsch,[2] Phil Holzmeister,[2]* Wooli Bae,[1] Luisa M. Kneer,[1] Dina Grohmann,[2]† Philip Tinnefeld,[2]‡ Tim Liedl[1]‡

Forces in biological systems are typically investigated at the single-molecule level with atomic force microscopy or optical and magnetic tweezers, but these techniques suffer from limited data throughput and their requirement for a physical connection to the macroscopic world. We introduce a self-assembled nanoscopic force clamp built from DNA that operates autonomously and allows massive parallelization. Single-stranded DNA sections of an origami structure acted as entropic springs and exerted controlled tension in the low piconewton range on a molecular system, whose conformational transitions were monitored by single-molecule Förster resonance energy transfer. We used the conformer switching of a Holliday junction as a benchmark and studied the TATA-binding protein–induced bending of a DNA duplex under tension. The observed suppression of bending above 10 piconewtons provides further evidence of mechanosensitivity in gene regulation.

The single-molecule force spectroscopy techniques that are most widely used to study minute forces and mechanical properties of biomolecules are atomic force microscopy and optical and magnetic tweezers. These methods have helped to explore the unfolding and folding of proteins (*1*, *2*), the elasticity of DNA (*3*), and the folding trajectory of proteins in force clamp configurations (*4*). Despite this success, two limitations persist. One is the low data throughput arising from the serial nature of conventional force spectroscopy. Recent attempts to overcome this problem include the development of increased parallel data acquisition in magnetic tweezer experiments (*5*) and centrifuge force microscopes (*6*). The second limitation is the requirement of a physical connector to a micrometer-sized object that enables interaction with the macroscopic world (*7*). These typically long and flexible connector molecules are an intrinsic feature of all established techniques and make them susceptible to drift and noise. Further, they prevent the investigation of DNA-interacting systems that induce only minor conformational changes, such as many gene-regulatory proteins (e.g., transcription factors). One previous attempt to reduce noise involved the use of DNA origami bundles as rigid spacers in optical traps (*8*). Regardless, any tether prohibits access to biologically relevant complex environments such as the inside of living cells.

A promising approach toward the complete removal of the invasive connection is the construction of autonomous, nanoscopic manipulation tools. Earlier efforts on the molecular scale to sense forces autonomously, although not in an adjustable fashion, include simple nanomechanical DNA devices (*9*–*11*) and intracellular protein force sensors (*12*). In this work, we used programmable DNA self-assembly (*13*–*18*) to construct a nanoscopic device that overcomes both limitations. Extending prestressed DNA origami tensegrity (*19*), we used the entropic spring behavior of single-stranded DNA (ssDNA) to exert defined and tunable forces on molecular systems. Conceptually, the ssDNA connects the system of interest with two immobile anchor points (Fig. 1A). By adjusting the number of bases between the fixed anchor points, the contour length of the ssDNA can be changed, directly affecting the entropic force acting on the system under study. The fixed distance imparted by the rigid DNA structure and the given contour length of the ssDNA provide an approximately constant force over time (supplementary text, section S1) (*20*). In analogy to the nomenclature of established constant-force experiments, we call our device a nanoscopic force clamp.

In the experimental realization, the ssDNA spring spans the gap of a rigid, bracket-shaped DNA origami clamp and is part of the long scaffold strand that forms the backbone of the DNA origami structure (Fig. 1B). For our design, we located the multiple cloning site (MCS) of the M13mp18 scaffold in the middle of the spring, which allowed us to insert and probe any DNA sequence of interest by means of standard cloning procedures. Additional ssDNA scaffold was stored in reservoir loops on both ends of the clamp. This enabled us to cost-efficiently build multiple objects with ssDNA springs of different lengths, permitting a flexible design with adjustable force (*19*). Individual structures were

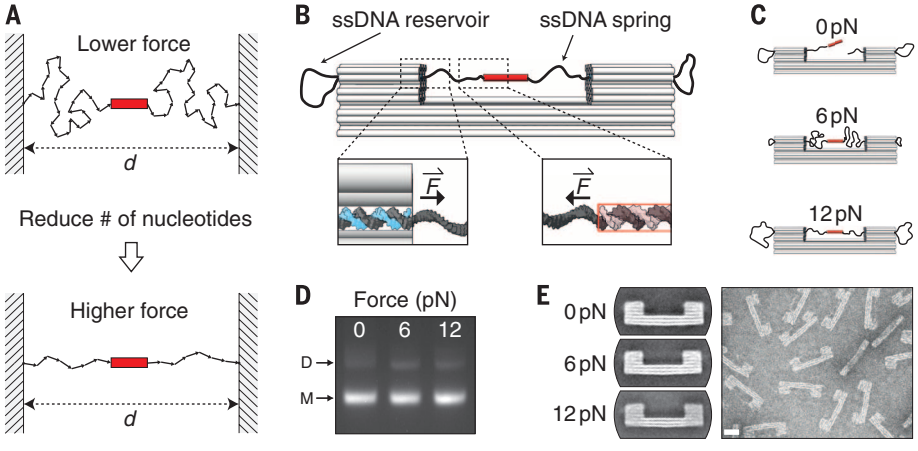

Fig. 1. DNA origami force clamp. (**A**) ssDNA connects the molecular system of interest (red rectangle) with two immobile anchor points. Reducing the number of nucleotides spanning the distance *d* leads to a smaller number of adoptable conformations of the ssDNA chain and thus results in a higher entropic force. (**B**) Structure of the DNA origami force clamp. ssDNA exits the clamp duplexes in a shear conformation (left inset; scaffold in dark gray and staple in blue) and spans the 43-nm gap. ssDNA reservoirs are located on each side of the clamp. The system of interest (here a DNA duplex) is probed in shear conformation (right inset; scaffold in dark gray and complementary DNA in light gray). *F*, force. (**C**) For each constant-force variant (three variants are shown here), individual origami samples were assembled. (**D**) Agarose gel of the three variants after annealing, with the monomer (M) and dimer (D) bands of the origami structure highlighted. (**E**) Average TEM micrographs of the three variants (left) and a single negative-stain TEM image of the 6-pN variant (right). Scale bar, 20 nm.

[1]Faculty of Physics and Center for NanoScience, Ludwig-Maximilians-Universität, Geschwister-Scholl-Platz 1, 80539 München, Germany. [2]Institut für Physikalische und Theoretische Chemie, Braunschweig Integrated Centre of Systems Biology, and Laboratory for Emerging Nanometrology, Technische Universität Braunschweig, Rebenring 56, 38106 Braunschweig, Germany.
*Present address: Bayer AG, Engineering and Technology, Enabling Technologies, Chempark E41, 51368 Leverkusen, Germany.
†Present address: Department of Biochemistry, Genetics and Microbiology, Institute of Microbiology, University of Regensburg, 93053 Regensburg, Germany. ‡Corresponding author. Email: p.tinnefeld@tu-braunschweig.de (P.T.); tim.liedl@physik.lmu.de (T.L.)

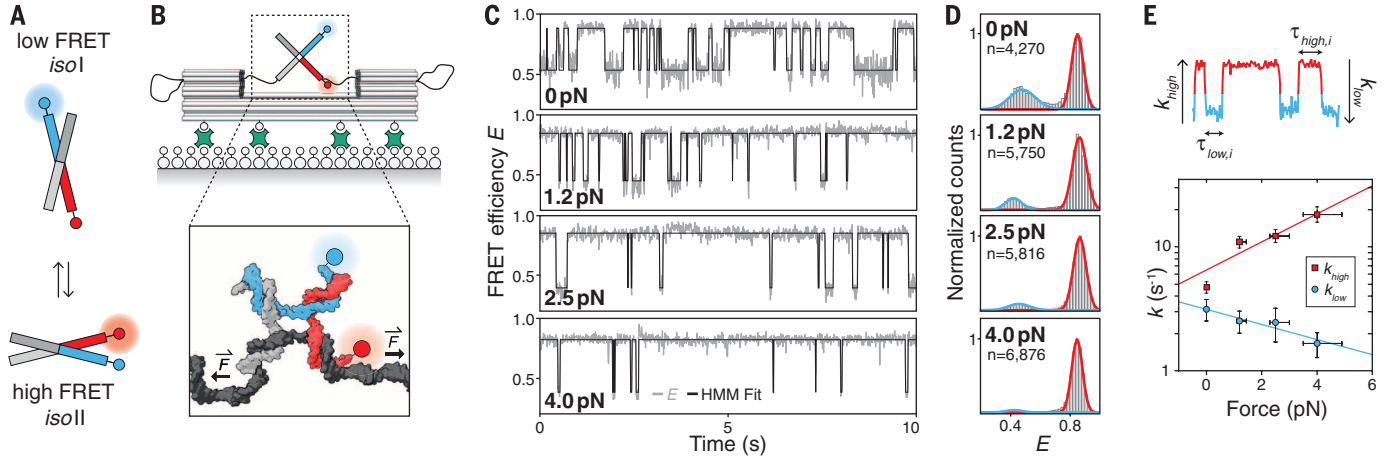

Fig. 2. Holliday junction conformer transitions under force. (**A**) Schematic of the Holliday junction (HJ) switching between two stacked isomers. Cy3 donor, blue; Cy5 acceptor, red. (**B**) Force clamps were immobilized on a bovine serum albumin–covered glass surface by biotin-streptavidin coupling. The HJ system is mounted in the force clamp with one of the four HJ strands being the scaffold (black strand in the inset). (**C**) FRET efficiency *E* traces (gray line) and two-state hidden Markov fit (HMM, black line). (**D**) Histograms over all recorded FRET traces, with Gaussian fits for the two FRET populations in blue (low FRET) and red (high FRET). Only traces with >20 transitions were included in the analysis; *n* is the total number of transitions. (**E**) Dwell times for both states ($\tau_{low,i}$ and $\tau_{high,i}$) were extracted for each trace. Transition rates (k_{low} and k_{high}) were first extracted from a monoexponential decay fit for each dwell time histogram, then averaged and plotted (semilog plot) as a function of force. Red squares, low to high FRET (k_{high}); blue circles, high to low FRET (k_{low}). Solid lines are exponential fits, where the exponent relates the rates to the applied force. The *y*-axis error is the standard error of each average rate; the *x*-axis error is the uncertainty of the calculated force (fig. S15).

assembled for each chosen length of the ssDNA spring with a distinct subset of only 10 oligonucleotides (staple strands) (Fig. 1C and figs. S1 to S3). For a zero-force control, we enzymatically cut the single-stranded spring to release any tension from the region of interest (Fig. 1C).

To calculate the resulting force for a given contour length, we approximated the ssDNA as a purely entropic spring by using a modified freely jointed chain model (*3*) with the contour length $L_C = N \times L_B$, with N being the number of nucleotides and L_B the length per single base (supplementary text, section S1). For L_B, we used 6.3 ± 0.8 Å, a value obtained from a length comparison of five different crystal structures of ssDNA segments (*21*).

We thermally annealed the force clamp structure, producing ~10^{12} force clamps in a single one-pot reaction. The chosen annealing ramp avoided temperatures above 65°C to minimize thermal degradation of the scaffold (fig. S4 and supplementary text, section S2) (*20*). We confirmed successful assembly by means of agarose gel electrophoresis (Fig. 1D and fig. S5), bulk Förster resonance energy transfer (FRET) experiments (fig. S6), and transmission electron microscopy (TEM) (Fig. 1E and figs. S7 to S13).

To demonstrate the functionality and sensitivity of our force clamp, we cloned a sequence into the scaffold that, together with three other oligonucleotides, forms the well-studied four-way Holliday junction (HJ) (*22*). In the presence of magnesium, the HJ forms an X-like structure by pairwise coaxial stacking of its helical arms. The chosen sequence is known to constantly switch between the two stacking conformers iso I and iso II (Fig. 2A) (*22*), a process that can be efficiently monitored with the help of a donor-acceptor FRET pair positioned on two of the arms (Fig. 2B and fig. S14). We chose four force variants ranging from 0 to 4.0 pN and confirmed their successful assembly (figs. S15 to S23). We immobilized these structures on a coverslip surface and monitored donor-acceptor pair intensities from individual force clamps over time in a confocal single-molecule setup with alternating laser excitation (ALEX) (*20*, *23*).

Exemplary FRET traces and FRET histograms from thousands of transitions are shown in Fig. 2, C and D, for each constant-force experiment (more traces are shown in figs. S24 and S25). A low-FRET population was centered at the FRET efficiency $E = 0.42$ (corresponding to iso I), and a high-FRET population was centered at $E = 0.85$ (corresponding to iso II). With increasing force, the equilibrium shifted toward the iso II conformation with almost no low-FRET population remaining at 4.0 pN. We used two-state hidden Markov modeling (*24*) to calculate the transition rates between the low- and high-FRET conformations for each of the forces. The transition rate from low to high FRET (k_{high}) increased from 4.7 ± 0.4 s^{-1} at 0 pN to 18.3 ± 1.4 s^{-1} at 4.0 pN. Meanwhile, the transition rate from high to low FRET (k_{low}) decreased from 3.2 ± 0.6 s^{-1} at 0 pN to 1.7 ± 0.4 s^{-1} at 4.0 pN (Fig. 2E). These rate changes are in good agreement with reported values from combined FRET and optical and magnetic tweezer measurements (*22*, *25*). Importantly, the heterogeneity of the HJ (*26*) was preserved in our measurements (fig. S26), indicating that the force clamp itself did not influence the dynamics of the HJ.

Next, we studied the force dependency of the TATA-binding protein (TBP)–induced bending of a DNA duplex. Such DNA distortions are an integral function of many transcription factors and DNA binding proteins. Although the correlation between transcriptional regulation and chromosome organization is well known, it has been challenging to quantify the impact of the DNA condensation state and the chromosome organization (e.g., the extent of strain in the DNA) on transcription factors such as TBP.

TBP is found in the archaeal and eukaryotic domains of life. It recognizes the minor groove of the adenine- and thymidine-rich TATA box in the core promoter sequence and introduces a severe ~90° bend in the DNA. Together with transcription factor B [TFB/TF(II)B], TBP is responsible for the site-specific recruitment and orientation of RNA polymerases at the transcription start site. To date, force measurements of this system have been futile, at least partly because the TBP-induced changes in the DNA topology are not easily detectable through the long tethers that are unavoidable in standard force spectroscopy experiments. Fluorescence readout in combination with our high-throughput method helped us to circumvent this problem.

We used TBP from the hyperthermophilic archaeal organism *Methanocaldococcus jannaschii* (MjTBP) (Fig. 3A), which bends the promoter DNA in one step without the need for the second transcription initiation factor TFB/TF(II)B (*27*), and inserted into the scaffold a promoter sequence, derived from the *Sulfolobus* spindle-shaped virus 1 (SSV) T6 gene promoter, that contains a TATA box motif and is recognized by MjTBP (Fig. 3B and fig. S27). We chose six force clamp variants ranging from 0 to 11.4 pN and confirmed their successful assembly (figs. S28 to S40). The complementary

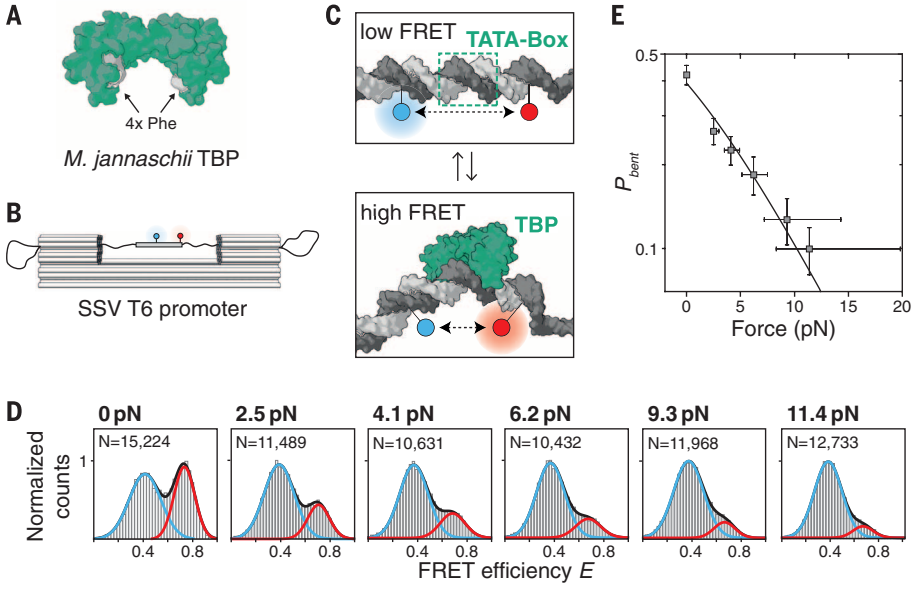

Fig. 3. TBP-induced DNA bending under force. (**A**) TBP from *M. jannaschii* (MjTBP; Protein Data Bank ID, 2Z8U) (*29*). Two pairs of phenylalanines (Phe) located in the DNA binding domain promote DNA bending. (**B**) The SSV T6 promoter, including the TATA box, mounted on the force clamp. Atto532 donor, blue; Atto647n acceptor, red. (**C**) TBP binds the minor groove of the TATA box and bends the duplex by almost 90°, thus changing the distance between the donor and acceptor. (**D**) FRET histograms and Gaussian fits for the low-FRET (blue) and high-FRET (red) populations. *N* is the number of molecules measured for each force. (**E**) Semilog plot of the probability of the bent state P_{bent} as a function of force. The solid line is a Boltzmann distribution fit. The *y*-axis error is the standard error of P_{bent}; the *x*-axis error is the uncertainty of the calculated force (fig. S28).

strand of the 51–base-pair–long SSV T6 promoter was hybridized to the scaffold during folding. Bending was monitored by single-molecule FRET measurements of a donor-acceptor pair flanking the TATA box (Fig. 3C and fig. S27). We chose in-solution over surface measurements to greatly increase the data acquisition throughput (*28*). Fluorescence bursts of the donor and acceptor were recorded before and after the addition of MjTBP.

Figure 3D shows histograms of the FRET efficiency with MjTBP for the six different forces. Each histogram includes data from at least 10,000 measured force clamps, although the average recording time per sample was only ~30 min. All histograms show a bimodal distribution with a low-FRET population centered at E = 0.42 (corresponding to the undistorted state) and a high-FRET population centered at E = 0.74 (corresponding to the bent state). The high-FRET population disappeared gradually with increasing force, and the TBP-induced bending was almost completely suppressed at 11.4 pN (full histograms for E and stoichiometry are shown in fig. S41). We calculated the probability of the bent state P_{bent} from its relative occurrence within the bimodal FRET distribution and plotted P_{bent} as a function of force (Fig. 3E). P_{bent} is well described by the difference in free energy between the unbent and bent states, expressed through a Boltzmann distribution (Fig. 3E and supplementary text, section S3) (*20*). An estimate of the change in binding affinity and Gibbs free energy is given in fig. S42.

Our DNA origami force clamp serves as a new tool to quantify the sensitivity of transcription factor–induced distortion to DNA tension and thus to chromosome organization. This adds information to the growing picture of transcriptional regulation and protein-DNA interactions in general. Our nanoscopic force clamp expands the range of available single-molecule force spectroscopy techniques and makes new molecular systems accessible to sensitive force spectroscopy analysis. The self-assembling clamps are easy to prepare and can be used to study any DNA-interacting and DNA-modifiable system (e.g., proteins conjugated with short DNA tethers). The simple operation and highly increased throughput compared with standard techniques facilitate the generation of force spectroscopy data in a dynamic range of 0 to 12 pN, which easily can be extended to ~50 pN (supplementary text, section S4) (*20*). Given that our method provides the flexibility to perform both on-surface and in-solution experiments, we envision moving from elaborate and costly single-molecule tools toward simple and readily adaptable ensemble assays.

REFERENCES AND NOTES

1. M. S. Kellermayer, S. B. Smith, H. L. Granzier, C. Bustamante, *Science* **276**, 1112–1116 (1997).
2. M. Rief, M. Gautel, F. Oesterhelt, J. M. Fernandez, H. E. Gaub, *Science* **276**, 1109–1112 (1997).
3. S. B. Smith, Y. Cui, C. Bustamante, *Science* **271**, 795–799 (1996).
4. J. M. Fernandez, H. Li, *Science* **303**, 1674–1678 (2004).
5. N. Ribeck, O. A. Saleh, *Rev. Sci. Instrum.* **79**, 094301 (2008).
6. K. Halvorsen, W. P. Wong, *Biophys. J.* **98**, L53–L55 (2010).
7. K. C. Neuman, A. Nagy, *Nat. Methods* **5**, 491–505 (2008).
8. E. Pfitzner *et al.*, *Angew. Chem. Int. Ed. Engl.* **52**, 7766–7771 (2013).
9. H. Shroff *et al.*, *Nano Lett.* **5**, 1509–1514 (2005).
10. W. Shen, M. F. Bruist, S. D. Goodman, N. C. Seeman, *Angew. Chem. Int. Ed. Engl.* **43**, 4750–4752 (2004).
11. H. Gu, W. Yang, N. C. Seeman, *J. Am. Chem. Soc.* **132**, 4352–4357 (2010).
12. C. Grashoff *et al.*, *Nature* **466**, 263–266 (2010).
13. N. C. Seeman, *Nature* **421**, 427–431 (2003).
14. P. W. K. Rothemund, *Nature* **440**, 297–302 (2006).
15. S. M. Douglas *et al.*, *Nucleic Acids Res.* **37**, 5001–5006 (2009).
16. Y. Ke *et al.*, *J. Am. Chem. Soc.* **131**, 15903–15908 (2009).
17. E. S. Andersen *et al.*, *Nature* **459**, 73–76 (2009).
18. S. M. Douglas *et al.*, *Nature* **459**, 414–418 (2009).
19. T. Liedl, B. Högberg, J. Tytell, D. E. Ingber, W. M. Shih, *Nat. Nanotechnol.* **5**, 520–524 (2010).
20. Materials and methods are available as supplementary materials on *Science* Online.
21. M. C. Murphy, I. Rasnik, W. Cheng, T. M. Lohman, T. Ha, *Biophys. J.* **86**, 2530–2537 (2004).
22. S. Hohng *et al.*, *Science* **318**, 279–283 (2007).
23. J. Ross *et al.*, *J. Phys. Chem. B* **111**, 321–326 (2007).
24. S. A. McKinney, C. Joo, T. Ha, *Biophys. J.* **91**, 1941–1951 (2006).
25. F. E. Kemmerich *et al.*, *Nano Lett.* **16**, 381–386 (2016).
26. C. Hyeon, J. Lee, J. Yoon, S. Hohng, D. Thirumalai, *Nat. Chem.* **4**, 907–914 (2012).
27. A. Gietl *et al.*, *Nucleic Acids Res.* **42**, 6219–6231 (2014).
28. A. N. Kapanidis *et al.*, *Acc. Chem. Res.* **38**, 523–533 (2005).
29. N. Adachi, M. Senda, R. Natsume, T. Senda, M. Horikoshi, *Genes Cells* **13**, 1127–1140 (2008).

ACKNOWLEDGMENTS

We thank H. Gaub, A. Gietl, A. Maier, I. MacPherson, J. Lipfert, M. Pilo-Pais, J. Rädler, O. Saleh, and T. Zhang for discussions and S. Kempter and G. Schwake for technical assistance. S. Schulz kindly prepared the MjTBP. This work was supported by the Deutsche Forschungsgemeinschaft [grant LI 1743/2-1, grant TI 329/6-1, grant GrK1952/1 ("Metrology for Complex Nanosystems"), Nanosystems Initiative Munich, grant SFB 1032 (TPA6), and grant SFB 960 (TPA7)], the Braunschweig International Graduate School of Metrology, the European Commission [Framework Programme 7–EScoDNA grant agreement no. 317110 and European Research Council grant agreement no. 336440 for ORCA (Optical Responses Controlled by DNA Assembly)], and the Boehringer Ingelheim Foundation. P.C.N., B.W., and P.H. performed the experiments. P.C.N., D.G., P.T., and T.L. designed the research. P.C.N., B.W., P.H., L.M.K., W.B., P.T., and T.L. analyzed the data. P.C.N. and W.B. prepared the figures. P.C.N., P.T., D.G., and T.L. wrote the manuscript. All authors edited the manuscript. The authors declare that they have no competing interests. Additional data described in this work can be found in the supplementary materials.

SUPPLEMENTARY MATERIALS

www.sciencemag.org/content/354/6310/305/suppl/DC1
Materials and Methods
Supplementary Text
Figs. S1 to S42
Custom M13mp18-Based Scaffold Sequences
References (*30*–*40*)

19 July 2016; accepted 6 September 2016
10.1126/science.aah5974

Science
AAAS

Molecular force spectroscopy with a DNA origami–based nanoscopic force clamp

Philipp C. Nickels, Bettina Wünsch, Phil Holzmeister, Wooli Bae, Luisa M. Kneer, Dina Grohmann, Philip Tinnefeld and Tim Liedl

(October 20, 2016)
Science **354** (6310), 305-307. [doi: 10.1126/science.aah5974]

Editor's Summary

Many tiny force sensors

Several techniques can measure forces on biomolecules, but the need to connect the molecule to the macroscopic world often limits the rate at which data can be taken. Nickels *et al.* created large arrays of nanoscale force sensors by using DNA origami structures. Single-stranded DNA molecules of different lengths attached to the molecule of interest acted as entropic springs, with shorter strands exerting more force. The authors used their setup to study the bending of DNA induced by the TATA-binding protein.

Science, this issue p. 305

Science (print ISSN 0036-8075; online ISSN 1095-9203) is published weekly, except the last week in December, by the American Association for the Advancement of Science, 1200 New York Avenue NW, Washington, DC 20005.